

Macro-microscopic mass formulae and nuclear mass predictions

G. Royer, M. Guilbaud, A. Onillon

► **To cite this version:**

G. Royer, M. Guilbaud, A. Onillon. Macro-microscopic mass formulae and nuclear mass predictions. Nuclear Physics A, Elsevier, 2010, 847, pp.24-41. 10.1016/j.nuclphysa.2010.06.014 . in2p3-00523244

HAL Id: in2p3-00523244

<http://hal.in2p3.fr/in2p3-00523244>

Submitted on 4 Oct 2010

HAL is a multi-disciplinary open access archive for the deposit and dissemination of scientific research documents, whether they are published or not. The documents may come from teaching and research institutions in France or abroad, or from public or private research centers.

L'archive ouverte pluridisciplinaire **HAL**, est destinée au dépôt et à la diffusion de documents scientifiques de niveau recherche, publiés ou non, émanant des établissements d'enseignement et de recherche français ou étrangers, des laboratoires publics ou privés.

Macro-microscopic mass formulae and nuclear mass predictions

G. Royer, M. Guilbaud, A. Onillon

*Laboratoire Subatech, UMR: IN2P3/CNRS-Université-Ecole des Mines,
4 rue A. Kastler, 44307 Nantes Cedex 03, France*

1

Abstract

Different mass formulae derived from the liquid drop model and the pairing and shell energies of the Thomas-Fermi model have been studied and compared. They include or not the diffuseness correction to the Coulomb energy, the charge exchange correction term, the curvature energy, different forms of the Wigner term and powers of the relative neutron excess $I = (N - Z)/A$. Their coefficients have been determined by a least square fitting procedure to 2027 experimental atomic masses [1]. The Coulomb diffuseness correction Z^2/A term or the charge exchange correction $Z^{4/3}/A^{1/3}$ term plays the main role to improve the accuracy of the mass formula. The Wigner term and the curvature energy can also be used separately but their coefficients are very unstable. The different fits lead to a surface energy coefficient of around 17-18 MeV. A large equivalent rms radius ($r_0 = 1.22 - 1.24$ fm) or a shorter central radius may be used. A rms deviation of 0.54 MeV can be reached between the experimental and theoretical masses. The remaining differences come probably mainly from the determination of the shell and pairing energies. Mass predictions of selected expressions have been compared to 161 new experimental masses and the correct agreement allows to provide extrapolations to masses of 656 selected exotic nuclei.

PACS: 21.10.Dr; 21.60.Ev; 21.60.Cs

Keywords: Mass formula, liquid drop model, Wigner term, curvature energy.

¹ E-mail:royer@subatech.in2p3.fr

1 Introduction

Predictions of masses of unknown nuclei far away from the β -stability valley may be tentatively performed from mass formulae working well for the known isotopes. Semi-macroscopic liquid drop models including the pairing effects have been firstly developed to reproduce the experimental nuclear masses [2,3]. Later on, these macroscopic-microscopic approaches have been developed, mainly the finite-range liquid drop model and the finite-range droplet model [4], to describe the masses and the fission, fusion and alpha [5] processes in taking into account the shell effects, the proximity energy and the nuclear deformations. Nuclear masses have also been reproduced accurately within the statistical Thomas-Fermi model with a Seyler-Blanchard effective interaction [6,7] and microscopic Hartree-Fock self-consistent theories using mean-fields and Skyrme or Gogny forces and pairing correlations [8–12] as well as relativistic mean field theories [13] or Garvey-Kelson relations [14].

All these recent macroscopic-microscopic approaches aiming at reproducing the nuclear binding energy and then the nuclear mass contain the usual volume, surface, Coulomb energy terms and the shell and pairing energies and include or not the diffuseness correction to the Coulomb energy, the charge exchange correction term, the curvature energy, a constant term, different forms of the Wigner term and different powers of the relative neutron excess $I = (N - Z)/A$. The purpose of the present work is, firstly, to determine the most efficient mass formulae to reproduce the most precisely known masses given in the 2003 atomic mass evaluation [1]. Four possible radii are considered to calculate the Coulomb energy : the equivalent rms radius deduced from the experimental charge radius [15], a central radius used to determine the proximity energy [16], a radius free to evolve to minimise the difference between the theoretical and experimental masses and a fixed r_0 value. Secondly, the mass predictions of the selected formulae are compared with 161 new known experimental masses. The agreement allows finally to provide extrapolated masses of 656 unknown realistic exotic nuclei and to compare with the data given in the 2003 atomic mass evaluation.

2 Macro-microscopic Liquid Drop Model binding energy

Different subsets of the following expansion of the nuclear binding energy in powers of $A^{-1/3}$ and $|I|$ have been studied :

$$B = a_v (1 - k_v I^2) A - a_s (1 - k_s I^2) A^{2/3} - a_k (1 - k_k I^2) A^{1/3} - \frac{3 e^2 Z^2}{5 R_0}$$

$$+f_p \frac{Z^2}{A} + a_{c,exc} \frac{Z^{\frac{4}{3}}}{A^{\frac{1}{3}}} - E_{pair} - E_{shell} - E_{Wigner}. \quad (1)$$

The volume energy corresponding to the saturated exchange force and infinite nuclear matter is given by the first term. I^2A is the asymmetry energy of the Bethe-Weizsäcker mass formula. The second term is the surface energy. Its origin is the deficit of binding energy of the nucleons at the nuclear surface and corresponds to semi-infinite nuclear matter. The following term is the curvature energy. It results from non uniform properties which correct the surface energy and depends on the mean local curvature. This term appears in the TF model [7] but vanishes in the FRLDM [4]. The decrease of binding energy due to the Coulomb repulsion is given by the fourth term. Different charge radii will be assumed. The Z^2/A term is the diffuseness correction to the sharp radius Coulomb energy (called also the proton form-factor correction in [4]). The $Z^{4/3}/A^{1/3}$ term is the charge exchange correction term. The pairing and shell energies of the recent Thomas-Fermi model [6,7] have been selected. Their dependence on the proximity of the proton and neutron magic numbers and on the parity is displayed on Figures 1 and 2. The shell effects add 12.84 MeV to the binding energy of ^{208}Pb , for example.

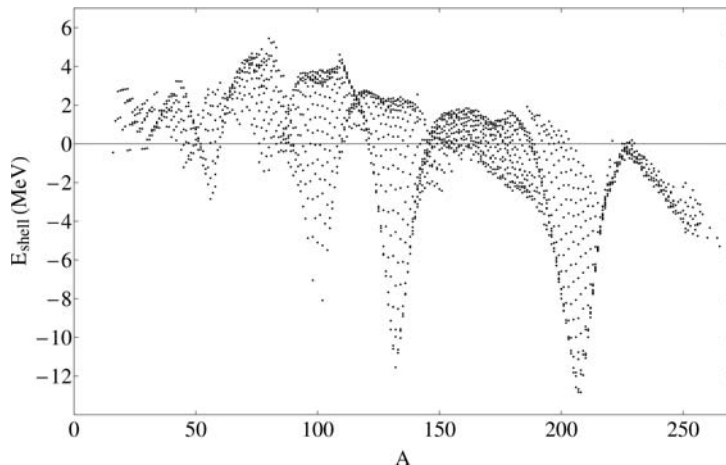


Fig. 1. Shell energies of the Thomas-Fermi model [7].

The Wigner energy appears in the counting of identical pairs in a nucleus and depends on I . Its effect is to decrease the binding energy when $N \neq Z$. Four versions of the Wigner term have been considered here, namely: the original linear version $W_1 = k_{w_1}|I|$, $W_2 = k_{w_2}|N - Z| \times e^{-(A/50)^2}$, $W_3 = k_{w_3}|N - Z| \times e^{-A/35}$ and $W_4 = k_{w_4}e^{-80I^2}$. W_2 and W_4 have been proposed in [17] but with different coefficients.

To obtain the coefficients of the selected expressions by a least square fitting procedure, the masses of the 2027 nuclei verifying the two conditions : N and Z higher than 7 and the one standard deviation uncertainty on the mass lower than or equal to 150 keV [1] have been used.

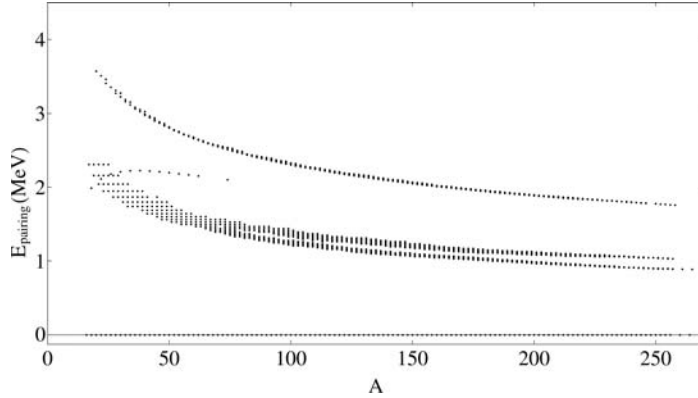


Fig. 2. Pairing energies of the Thomas-Fermi model [7].

3 Dependence on the Coulomb radius

In a previous study [18] it has been shown that, when the Coulomb reduced radius r_0 is a priori free and adjusted on the experimental masses as the other coefficients of the mass formulae, the adjustment leads always to a large value of around 1.21 – 1.255 fm.

To complete this study, the coefficients of different mass formulae have been adjusted, assuming a priori a specific expression for the Coulomb energy. Firstly, the Coulomb radius has been calculated using the expression $R_0 = 1.28A^{1/3} - 0.76 + 0.8A^{-1/3}$ (see Table 1). This formula proposed in Ref. [16] is derived from the droplet model and the proximity energy and simulates rather a central radius for which $R_0/A^{1/3}$ increases slightly with the mass. This radius is much smaller than the equivalent rms radius for which the experimental value of $R_0/A^{1/3}$ decreases slightly with the mass [15,19] and has an isospin dependence and a mean value of 1.2257 fm. It has been shown [5,20] that this selected more elaborated expression can also be used to reproduce accurately the fusion, fission and cluster and alpha decay data. The main result is that a rms deviation of only 0.56 MeV can be reached within seven adjustable parameters.

In Table 2 the assumed charge radius is simply $R_0 = 1.16A^{1/3}$ fm. This often used mean value does not allow to reach an accuracy better than 0.72 MeV. The surface coefficient is generally higher. So it seems that a large equivalent rms radius or a very low central Coulomb radius may be used in the mass formulae but that an intermediate radius is less efficient.

The values of the parameters and their correlations are discussed in the next section.

Table 1

Coefficient values and root mean square deviation (in MeV) between the theoretical and experimental binding energies. The theoretical shell and pairing energies are taken into account. The Coulomb energy is determined by $0.6e^2Z^2/(1.28A^{1/3} - 0.76 + 0.8A^{-1/3})$.

a_v	k_v	a_s	k_s	f_p	$a_{c,exc}$	W_1	W_2	W_3	W_4	σ
15.8548	1.7281	17.3228	0.8179	-	-	-	-	-	-	1.402
15.8427	1.7368	17.2607	0.8727	-	-	-	0.4083	-	-	1.368
15.8276	1.7681	17.176	1.0540	-	-	-	-	1.1872	-	1.334
15.8328	1.8931	17.1077	1.9361	-	-	41.003	-	-	-	1.199
16.038	1.9801	18.4563	2.2201	-	-	-	-	-	-8.4670	0.994
15.5172	1.7753	17.9474	1.6575	2.1401	-	-	-	-	-	0.692
15.2508	1.7840	17.9475	1.6577	-	2.0195	-	-	-	-	0.691
15.6233	1.8412	18.1709	1.92097	1.7987	-	-	-	-	-2.4136	0.661
15.3989	1.8492	18.1703	2.0320	-	1.6983	-	-	-	-2.4059	0.661
15.5002	1.7860	17.8829	1.7290	2.1612	-	-	0.4645	-	-	0.597
15.2312	1.7949	17.8831	1.7291	-	2.0393	-	0.4641	-	-	0.596
15.5003	1.8088	17.8136	1.8401	2.1032	-	-	-	0.9951	-	0.591
15.5389	1.8585	17.7736	2.1451	1.9299	-	21.437	-	-	-	0.591
15.2986	1.8690	17.7739	2.1444	-	1.8212	21.401	-	-	-	0.590
15.5899	1.8840	17.9004	2.2326	1.7779	-	19.554	-	-	-1.2050	0.583
15.3684	1.8924	17.9003	2.2316	-	1.6783	19.528	-	-	-1.2004	0.582
15.5868	1.8602	18.0012	2.0434	1.8294	-	-	-	0.9428	-1.9495	0.567
15.3587	1.8687	18.0007	2.0427	-	1.7272	-	-	0.9424	-1.9425	0.567
15.6096	1.8543	18.1132	2.0021	1.80856	-	-	0.4700	-	-2.4953	0.558
15.3841	1.8625	18.1127	2.0014	-	1.7073	-	0.4696	-	-2.4886	0.558

4 Correlations between the LDM parameters

The correlations between the different terms of the semi-empirical LDM mass formulae have been deeply investigated by M.W. Kirson [21] using correlation and error matrix starting directly from the four basic terms of the Bethe-Weizsäcker mass formula (see also [22]). Here I^2A is called the symmetry term and $I^2A^{2/3}$ the surface symmetry term.

Let us first recall the main conclusions of this study [21]. There is not much correlation of the volume, Coulomb, pairing and shell correction terms with other terms. The shell correction term is the most important single term to be added to the initial Bethe-Weizsäcker mass formula followed by the surface symmetry contribution. The pairing term is remarkably stable and there is essentially no correlation between the pairing term and any other term. The surface symmetry term is always important but less so when a wigner

term is present. The inclusion of the curvature term may seem questionable. Significant correlation exists between symmetry and exchange Coulomb term ($Z^{4/3}/A^{1/3}$ term), between surface and curvature terms and between Wigner and surface symmetry terms. The drastically variable terms are the Wigner and curvature terms for which even their sign is not definite. It is tempting to rule out any mass formula which does not contain a surface symmetry term. The direct and exchange Coulomb terms are anti-correlated. There is no compelling reason to introduce a congruence term to forego the linear form of the Wigner term as there is no compelling reason to prefer a non-linear form of the surface symmetry term to the linear form.

As recommended in this study, all the recent versions of the liquid drop model [4,20,23] contain a symmetry term, a surface symmetry term and shell and pairing corrections. The fact that the shell and pairing energies are uncorrelated with the other macroscopic terms justifies the possibility to select specific shell energies and formulae for the pairing corrections.

The analyzes of the tables in Ref. [18] and of the tables 1 and 2 of the present work are in agreement with all the above mentioned conclusions. The shell corrections of the Thomas-Fermi model selected in our approach go beyond simple coarse-grained global analytical shell corrections. This leads to a large improved accuracy and allows to extract the following supplementary information from the tables 1 and 2 and from [18]. The correlation between the Coulomb diffuseness correction term and the surface energy term is the same as the one between the charge exchange correction term and the surface energy term. The diffuseness correction term (in Z^2/A) has the advantage to be continuous during the transition from one-body to two-body shapes, at least in symmetric exit or entrance channels. The diffuseness correction term or the charge exchange correction term plays the main role to improve the accuracy of the mass formulae. The W_2 and W_3 terms are as efficient as the usual W_1 term when the diffuseness correction term is added. The convergency of the coefficients of the W_2 and W_3 terms is better than the one of the W_1 term. The introduction of a Coulomb diffuseness correction term divides W_1 by two and vanishes the efficiency of the curvature correction term.

The parameters of the LDM mass formula probably lie in the following range of values : $a_v = 15.3 - 15.9$ MeV, $a_s = 16.5 - 18.5$ MeV, $k_v = 1.7 - 1.9$, $k_s = 1.4 - 2.8$, $r_0 = 1.20 - 1.25$ fm, $f_p = 0.9 - 2.2$, $W_1 = 16 - 42$ MeV, $W_2 = 0.45 - 0.5$ MeV, $W_3 = 0.9 - 1.3$ MeV and $W_4 = 1.2 - 2.5$ MeV.

Let us recall that it has been previously shown that an $|I|$ or I^4 dependence in the surface and volume energies improves only slightly the efficiency of the expansion and that the introduction of a constant term is difficult since its value is highly fluctuating while a congruence term leads to high discontinuities at the scission point of fission or fusion barriers. The surface coefficient

and the relative radius r_0 are correlated since r_0 diminishes when the surface coefficient increases.

Table 2

Same as Table 1 but the Coulomb energy is determined by $0.6e^2Z^2/(1.16A^{1/3})$.

a_v	k_v	a_s	k_s	f_p	$a_{c,exc}$	W_1	W_2	W_3	W_4	σ
16.0975	1.6145	18.4883	0.3684	-	-	-	-	-	-	1.757
16.1273	1.5934	18.642	0.2466	-	-	-	-1.0105	-	-	1.583
16.1388	1.5552	18.711	0.0449	-	-	-	-	-1.8053	-	1.631
16.1017	1.5836	18.5293	0.1728	-	-	-7.8076	-	-	-	1.751
16.3374	1.9404	19.9732	2.0989	-	-	-	-	-	-11.0907	1.186
15.7511	1.6597	19.1291	1.1916	2.1955	-	-	-	-	-	1.233
15.4781	1.6665	19.129	1.1914	-	2.0710	-	-	-	-	1.233
16.0616	1.8498	19.7833	1.9150	1.1963	-	-	-	-	-7.0645	1.079
15.9131	1.8552	19.7832	1.9149	-	1.1278	-	-	-	-7.0659	1.079
15.7862	1.6384	19.2616	1.0584	2.1520	-	-	-0.9546	-	-	1.001
15.5185	1.6457	19.2616	1.0583	-	2.0302	-	-0.9550	-	-	1.001
15.7855	1.5936	19.3991	0.8600	2.2700	-	-	-	-2.0089	-	0.996
15.7174	1.5313	19.3998	0.5023	2.5229	-	-33.3855	-	-	-	1.098
15.4034	1.5363	19.4002	0.5014	-	2.3807	-33.4319	-	-	-	1.098
16.1454	1.7460	20.4634	1.2294	1.2486	-	-49.1756	-	-	-10.1039	0.739
15.9900	1.7505	20.4634	1.2289	-	1.1782	-49.1935	-	-	-10.1026	0.739
16.1478	1.8064	20.1843	1.6570	1.1238	-	-	-	-2.2277	-8.161	0.722
16.0082	1.8058	20.1842	1.6568	-	1.0597	-	-	-2.2280	-8.1614	0.722
16.0889	1.8245	19.8986	1.7673	1.1767	-	-	-0.9394	-	-6.9010	0.814
15.9426	1.8295	19.8984	1.7670	-	1.1098	-	-0.9397	-	-6.9003	0.814

5 Different possible mass formulae

The following formulae (2-6) have been obtained assuming the proportionality of R_0 with $A^{1/3}$ but the reduced radius r_0 is provided as the other coefficients by the adjustment to the experimental masses. The rms deviations are respectively : 0.633, 0.579, 0.610, 0.564 and 0.543 MeV. The Wigner terms are more efficient than the curvature term but they induce a high value of r_0 . The combination of two Wigner terms allows to reach a very good accuracy. Nevertheless the formula (2) with only 6 parameters and without Wigner terms already leads to a correct precision.

$$B = 15.4122 \left(1 - 1.7116I^2\right) A - 17.5371 \left(1 - 1.4015I^2\right) A^{\frac{2}{3}} - 0.6 \frac{e^2 Z^2}{1.2177 A^{\frac{1}{3}}}$$

$$+1.3736 \frac{Z^2}{A} - E_{pair} - E_{shell}. \quad (2)$$

$$B = 15.3529 (1 - 1.8084I^2) A - 16.9834 (1 - 1.9647I^2) A^{\frac{2}{3}} - 0.6 \frac{e^2 Z^2}{1.2324A^{\frac{1}{3}}} \\ + 0.9675 \frac{Z^2}{A} - 21.3975|I| - E_{pair} - E_{shell}. \quad (3)$$

$$B = 15.4529 (1 - 1.8722I^2) A - 18.0588 (1 - 2.7716I^2) A^{\frac{2}{3}} - 0.6 \frac{e^2 Z^2}{1.2204A^{\frac{1}{3}}} \\ + 1.3712 \frac{Z^2}{A} + 1.348 (1 - 45.I^2) A^{\frac{1}{3}} - E_{pair} - E_{shell}. \quad (4)$$

$$B = 15.2508 (1 - 1.7489I^2) A - 16.8015 (1 - 1.6077I^2) A^{\frac{2}{3}} - 0.6 \frac{e^2 Z^2}{1.2426A^{\frac{1}{3}}} \\ + 1.0736 \frac{Z^2}{A} - 0.6806|N - Z| \times e^{-(A/50)^2} - E_{pair} - E_{shell}. \quad (5)$$

$$B = 15.4133 (1 - 1.7962I^2) A - 17.3079 (1 - 1.7858I^2) A^{\frac{2}{3}} - 0.6 \frac{e^2 Z^2}{1.2318A^{\frac{1}{3}}} \\ + 0.8956 \frac{Z^2}{A} - 0.4838|N - Z| \times e^{-(A/50)^2} + 2.2 \times e^{-80I^2} - E_{pair} - E_{shell}. \quad (6)$$

Experimentally for nuclei verifying N and Z higher than 7 the set of 782 ground state nuclear charge radii presented in ref. [15] leads for the equivalent rms charge radius given by $R_0 = \sqrt{(5/3)} \langle r^2 \rangle^{1/2}$ to $R_0 = 1.22572 A^{1/3}$ fm and $\sigma = 0.124$ fm. This radius value is imposed in the formula (7). It allows also to obtain a good accuracy of 0.584 MeV.

$$B = 15.3848 (1 - 1.7837I^2) A - 17.1947 (1 - 1.8204I^2) A^{\frac{2}{3}} - 0.6 \frac{e^2 Z^2}{1.2257A^{\frac{1}{3}}} \\ + 1.1035 \frac{Z^2}{A} - 16.606|I| - E_{pair} - E_{shell}. \quad (7)$$

In the last formula (8) the radius is taken as the central radius previously used in Table 1 and $\sigma = 0.558$ MeV. So it is possible to obtain accurate mass

formulae with a large constant reduced radius r_0 or with a more sophisticated central radius corresponding to a smaller value of r_0 increasing with the mass.

$$\begin{aligned}
B = & 15.6096 \left(1 - 1.8543I^2\right) A - 18.1132 \left(1 - 2.0021I^2\right) A^{\frac{2}{3}} \\
& - 0.6 \frac{e^2 Z^2}{1.28A^{\frac{1}{3}} - 0.76 + 0.8A^{-\frac{1}{3}}} + 1.8086 \frac{Z^2}{A} - 0.47|N - Z| \times e^{-(A/50)^2} \\
& + 2.4954 \times e^{-80I^2} - E_{pair} - E_{shell}. \quad (8)
\end{aligned}$$

The Wigner energy terms are supposed to be approximately independent of the nuclear shape and they may induce discontinuities at the scission point of fission or fusion barriers. For example for symmetric decay of ^{254}Fm , the expressions $20|I|$, $0.4|N - Z| \times e^{-(A/50)^2}$, $|N - Z| \times e^{-A/35}$, $2e^{-80I^2}$ and $E_{cong} = -10e^{-4.2|I|}$ lead to discontinuities at the contact point of the nascent fragments of respectively 4.25, 0.03, 1.4, 0.05 and 4.1 MeV.

The difference between the theoretical masses calculated with the formulae (2-4,6-8) and the experimental masses of the 2027 selected nuclei are given from the top left to the bottom right on the Figure 3 as a function of the mass number. The structure observed in the whole data are about the same for the different formulae. They come probably mainly from the assumed shell and pairing energies. The errors are more important for the lighter nuclei. The mass of the heaviest nuclei is better reproduced by the formulae (2), (4) and (7). The formula (6) is the best one for the light nuclei while the formula (8) is a good compromise. As an illustration, the difference between the theoretical masses obtained with the formula (8) and the experimental masses of the 2027 nuclei used for the adjustment of the coefficients is indicated in Figure 4. The more the colour is dark the more the accuracy is high. The other formulae lead to similar pictures. The distribution of the nuclei in each error range is given explicitly in Figure 5. The errors are slightly larger for the light nuclei. The same behaviour is encountered by all the mass models. Nevertheless the error is very rarely higher than 2 MeV.

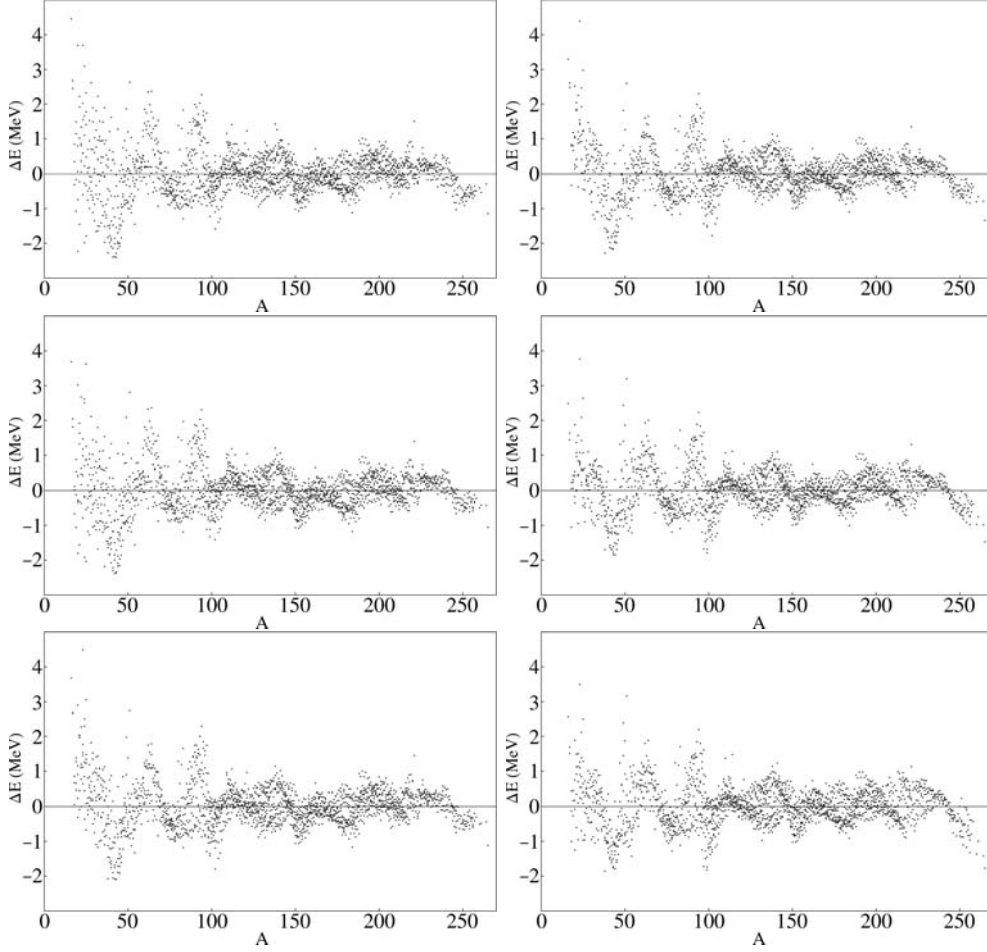


Fig. 3. Difference between the theoretical and experimental masses of the 2027 selected nuclei for the formulas (2-4,6-8) from the top left to the bottom right as a function of the mass number.

6 Test of the predictability on 161 new experimental masses

Since the last mass evaluation [1] other masses have been newly or more precisely obtained. The predictions given by the formulae (6-8) (not readjusted) are compared in Figure 6 with 161 new experimental masses for which the one standard deviation uncertainty is lower than or equal to 800 keV [1,24]. The accuracy is correct in the whole mass range showing the predictability of such formulae. The rms deviations are respectively 0.937, 0.985 and 0.976 MeV.

The location of these 161 nuclei as a function of their neutron and proton numbers is displayed in Figure 7 as the difference between the theoretical masses calculated from the formula (8) and the experimental ones. These new data are well distributed around the better known masses.

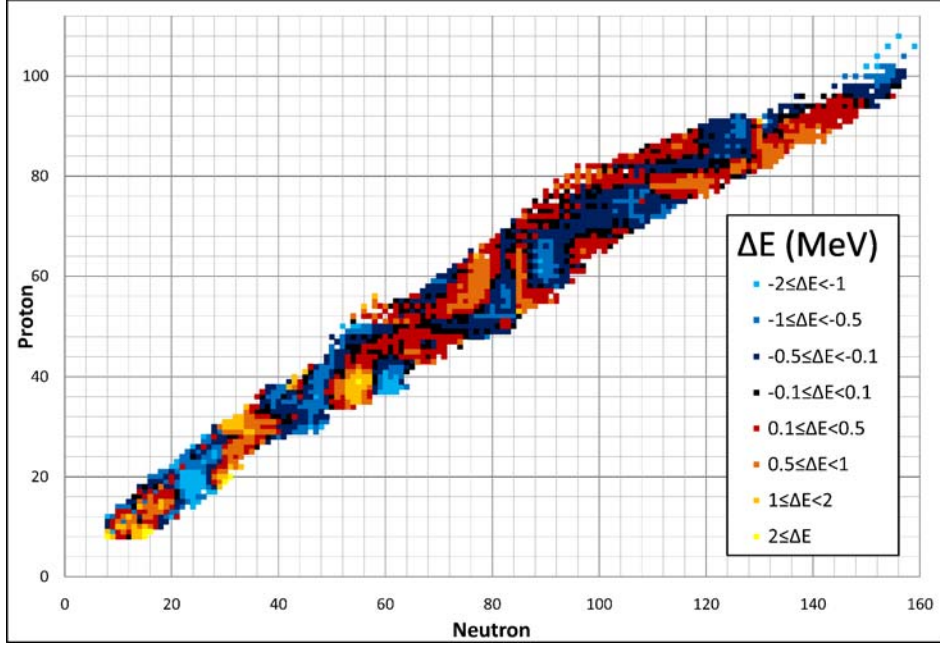


Fig. 4. Difference between the theoretical masses obtained with the formula (8) and the experimental masses of the 2027 selected nuclei.

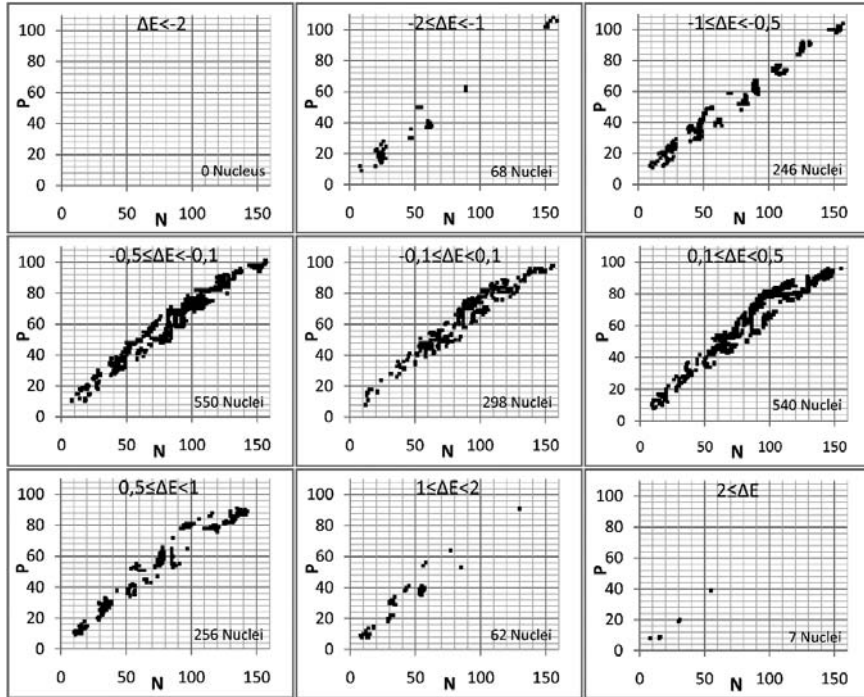


Fig. 5. Distribution of the 2027 nuclei in each error range.

The experimental mass excess for these nuclei is given in Table 3 as well as the difference between the mass excess derived from the formula (8) and the experimental ones for these 161 new nuclei.

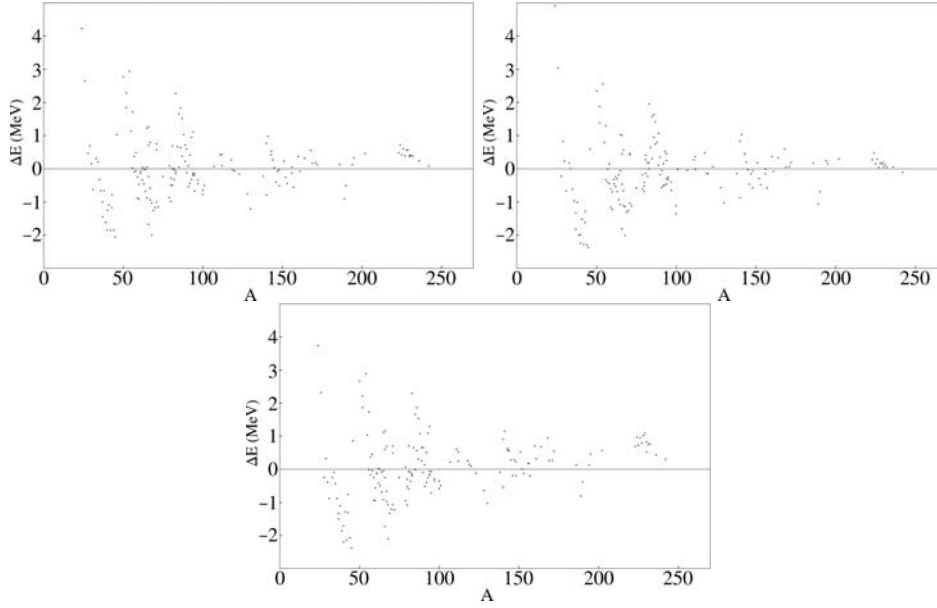


Fig. 6. Difference between the theoretical masses given by the formulas (6-8) and the experimental masses of 161 newly known nuclei.

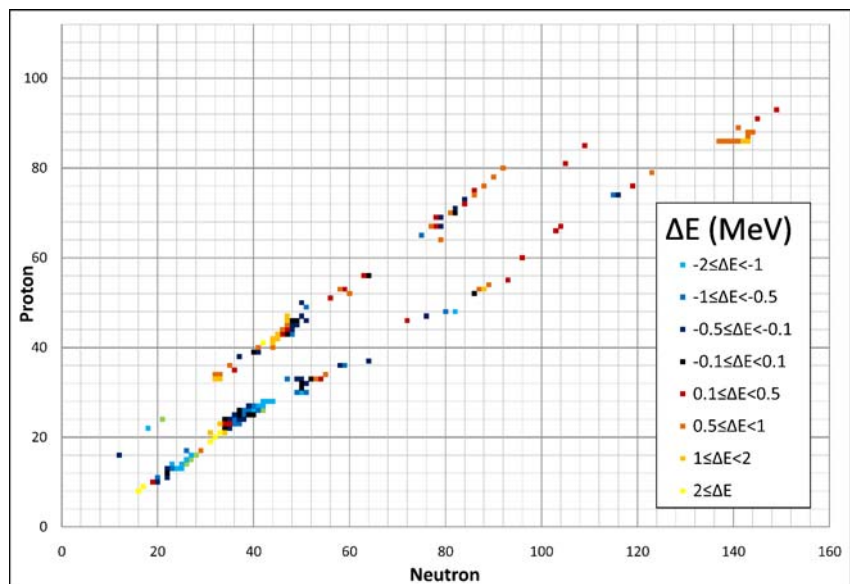


Fig. 7. Difference between the theoretical masses obtained with the formula (8) and the 161 new experimental masses.

7 Mass predictions for 656 exotic nuclei

Finally, the predictions for 656 other more exotic nuclei for which the mass is still unknown are compared to the extrapolations given in Ref. [1] with an assumed uncertainty often higher than 500 keV. Firstly, the predictions given by the formulae (6-8) (not readjusted) are compared in Figure 8 with these new 656 extrapolated masses. The rms deviation are respectively 1.011,

Table 3

Experimental mass excess (in MeV) and difference δE between the values predicted with the formula (8) and these new 161 experimental data.

Nucleus	E_{exp}	δE	Nucleus	E_{exp}	δE	Nucleus	E_{exp}	δE	Nucleus	E_{exp}	δE	Nucleus	E_{exp}	δE
²⁴ O	19.07	3.74	²⁶ F	18.27	2.32	²⁸ S	4.07	-0.25	²⁹ Ne	18.06	0.32	³⁰ Ne	23.1	-0.39
³¹ Na	12.65	-0.88	³³ Na	24.89	-0.24	³⁴ Mg	8.81	-0.09	³⁵ Al	-0.13	-0.43	³⁶ Al	5.78	-0.88
³⁷ Si	-6.58	-1.51	³⁷ Al	9.95	-1.34	³⁸ Al	16.05	-1.11	³⁹ Si	1.93	-1.87	⁴⁰ Ti	-8.85	-1.72
⁴⁰ Si	5.47	-2.2	⁴¹ P	-5.28	-1.29	⁴² P	0.94	-2.13	⁴³ S	-11.97	-1.31	⁴³ Cl	-24.17	-0.76
⁴⁴ S	-9.12	-2.07	⁴⁵ Cr	-18.97	-2.39	⁴⁶ Cl	-14.71	0.86	⁵⁰ K	-25.35	2.67	⁵² Sc	-40.36	1.87
⁵² Ca	-32.51	2.21	⁵⁴ Sc	-34.22	2.88	⁵⁵ Sc	-29.58	1.03	⁵⁶ Ti	-38.94	-0.02	⁵⁶ V	-46.8	1.74
⁵⁷ V	-44.19	0.37	⁵⁷ Ti	-33.54	-0.17	⁵⁸ V	-40.21	0.45	⁵⁸ Cr	-51.83	-0.04	⁵⁹ Cr	-47.89	-0.25
⁵⁹ V	-37.07	-0.94	⁶⁰ Cr	-46.5	-0.94	⁶⁰ V	-32.58	-0.56	⁶¹ Cr	-42.18	-0.12	⁶¹ Mn	-51.56	-0.13
⁶² Mn	-48.04	0.02	⁶² Cr	-40.41	-0.42	⁶³ Mn	-46.35	-0.5	⁶³ Fe	-55.63	0.00	⁶⁴ Mn	-42.62	-0.08
⁶⁴ Fe	-54.97	-0.69	⁶⁵ Mn	-40.67	-0.05	⁶⁵ Fe	-51.22	-0.91	⁶⁵ As	-46.78	1.11	⁶⁶ Fe	-49.57	-1.73
⁶⁶ As	-51.5	1.16	⁶⁶ Co	-56.41	-0.25	⁶⁶ Se	-41.83	0.6	⁶⁷ Fe	-45.69	-0.67	⁶⁷ Co	-55.06	-0.97
⁶⁷ Se	-46.55	0.69	⁶⁸ Fe	-43.13	-2.1	⁶⁸ Co	-51.35	-1.08	⁶⁹ Co	-50.00	-1.33	⁷⁰ Ni	-59.15	-1.21
⁷¹ Ni	-55.2	-1.07	⁷¹ Br	-57.06	0.49	⁷¹ Kr	-46.92	0.7	⁷² Ni	-53.94	-1.23	⁷⁵ Sr	-46.62	-0.25
⁷⁹ Y	-58.36	0.07	⁷⁹ Zn	-53.44	-0.96	⁸⁰ Zn	-51.65	-1.09	⁸⁰ As	-72.21	-0.53	⁸⁰ Y	-61.14	-0.3
⁸¹ Ga	-57.98	-0.07	⁸¹ Zr	-58.49	0.7	⁸¹ Zn	-46.2	-0.6	⁸² As	-70.32	-0.36	⁸² Ge	-65.58	-0.09
⁸³ Nb	-58.96	2.29	⁸³ Ge	-60.8	-0.15	⁸³ As	-69.56	-0.2	⁸⁴ Zr	-71.42	0.65	⁸⁵ Nb	-67.15	1.66
⁸⁵ As	-63.24	-0.02	⁸⁶ Mo	-64.56	1.86	⁸⁶ As	-58.96	0.57	⁸⁷ Mo	-67.69	1.53	⁸⁷ As	-55.62	0.31
⁸⁸ Tc	-61.68	1.07	⁸⁹ Ru	-58.99	0.65	⁸⁹ Tc	-67.39	0.26	⁹⁰ Tc	-70.72	-0.09	⁹⁰ Ru	-64.88	0.66
⁹¹ Tc	-75.98	-0.52	⁹¹ Ru	-68.24	0.13	⁹² Ru	-74.3	-0.39	⁹² Rh	-63.00	0.5	⁹³ Rh	-69.01	-0.26
⁹³ Pd	-59.44	1.09	⁹⁴ Kr	-61.35	-0.17	⁹⁴ Rh	-72.91	-0.15	⁹⁴ Pd	-66.1	-0.06	⁹⁴ Ag	-53.33	1.3
⁹⁵ Kr	-56.16	-0.71	⁹⁵ Pd	-69.96	-0.07	⁹⁷ Pd	-77.8	-0.29	⁹⁷ Ag	-70.82	-0.35	¹⁰⁰ In	-64.17	-0.59
¹⁰⁰ Sn	-56.78	-0.37	¹⁰¹ Rb	-43.6	-0.5	¹⁰⁷ Sb	-70.66	0.22	¹¹¹ I	-64.97	0.6	¹¹² Te	-77.57	0.53
¹¹² I	-67.06	0.24	¹¹⁸ Pd	-75.47	0.26	¹¹⁹ Ba	-64.59	0.14	¹²⁰ Ba	-68.89	0.09	¹²³ Ag	-69.38	-0.12
¹²⁸ Cd	-67.29	-0.65	¹³⁰ Cd	-61.57	-1.03	¹³⁸ Te	-65.76	-0.09	¹⁴⁰ Tb	-50.48	-0.54	¹⁴⁰ I	-63.6	0.9
¹⁴¹ I	-60.3	1.15	¹⁴³ Gd	-68.23	0.62	¹⁴³ Xe	-60.25	0.58	¹⁴⁴ Ho	-44.61	0.55	¹⁴⁵ Ho	-49.12	0.28
¹⁴⁶ Ho	-51.24	-0.19	¹⁴⁷ Tm	-35.97	0.29	¹⁴⁸ Cs	-47.3	0.23	¹⁴⁸ Tm	-38.77	-0.19	¹⁵¹ Yb	-41.54	0.53
¹⁵² Yb	-46.31	0.00	¹⁵³ Lu	-38.41	-0.13	¹⁵⁶ Nd	-60.53	0.18	¹⁵⁶ Hf	-37.85	0.17	¹⁵⁷ Ta	-29.63	-0.2
¹⁶⁰ W	-29.36	0.7	¹⁶¹ Re	-20.88	0.31	¹⁶⁴ Os	-20.46	0.68	¹⁶⁸ Pt	-11.04	0.95	¹⁶⁹ Dy	-55.6	0.26
¹⁷¹ Ho	-54.52	0.27	¹⁷² Hg	-1.09	0.55	¹⁸⁶ Tl	-20.19	0.13	¹⁸⁹ W	-35.48	-0.81	¹⁹⁰ W	-34.3	-0.39
¹⁹⁴ At	-1.19	0.13	¹⁹⁵ Os	-29.69	0.46	²⁰² Au	-24.4	0.56	²²³ Rn	20.4	0.69	²²⁴ Rn	22.44	0.97
²²⁵ Rn	26.56	0.72	²²⁶ Rn	28.74	0.95	²²⁷ Rn	32.88	0.79	²²⁸ Rn	35.25	1.01	²²⁹ Rn	39.36	1.08
²³⁰ Ac	33.81	0.53	²³⁰ Fr	39.5	0.83	²³¹ Ra	38.23	0.75	²³² Ra	40.5	0.77	²³⁶ Pa	45.35	0.43
²⁴² Np	57.42	0.3												

1.067 and 1.065 MeV. The global behaviour is similar. For about 50% of nuclei the difference is lower than 0.5 MeV and for 80% of nuclei the difference is lower than 1 MeV. The formula (7) is slightly closer to the 2003 AME predictions for the heaviest nuclei but for which the uncertainties are larger. These comparisons seem to confirm that this is the microscopic part of the

mass formulae which induces these structures in ΔE . The location of these

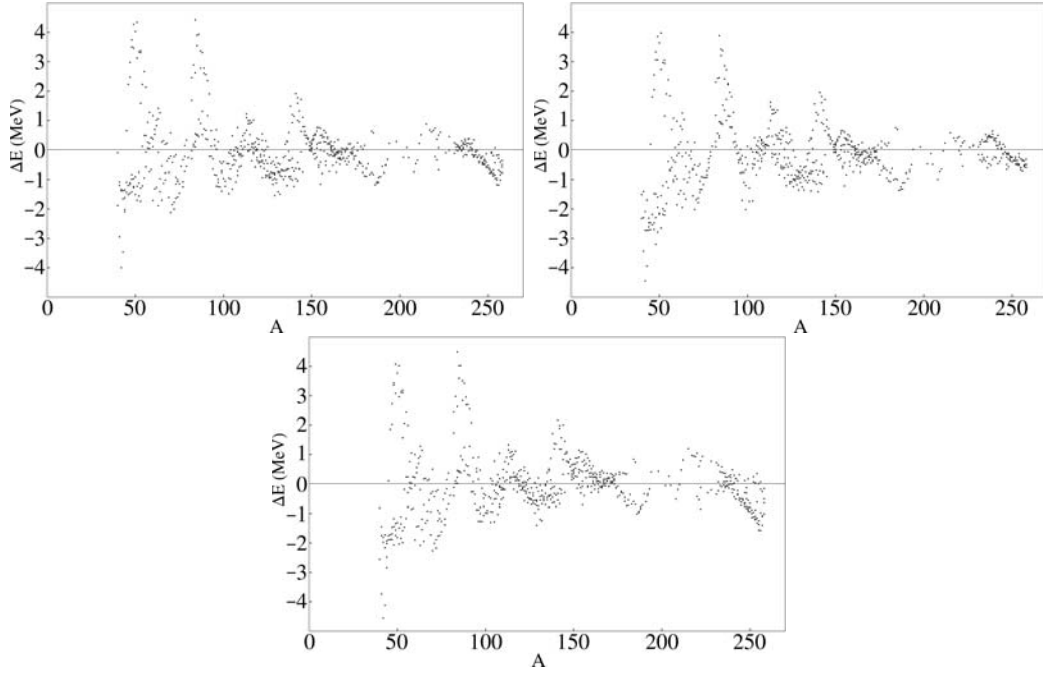


Fig. 8. Difference between the theoretical and AME extrapolated masses for the 656 nuclei and the formulae (6-8) from the top left to the bottom.

656 nuclei around the known valley of isotopes and the difference between the theoretical masses calculated from the formula (8) and the 2003 AME ones is displayed in Figure 9. Similar pictures are obtained using the formulae (6-7). The theoretical mass excesses predicted with the formula (8) and 2003 AME

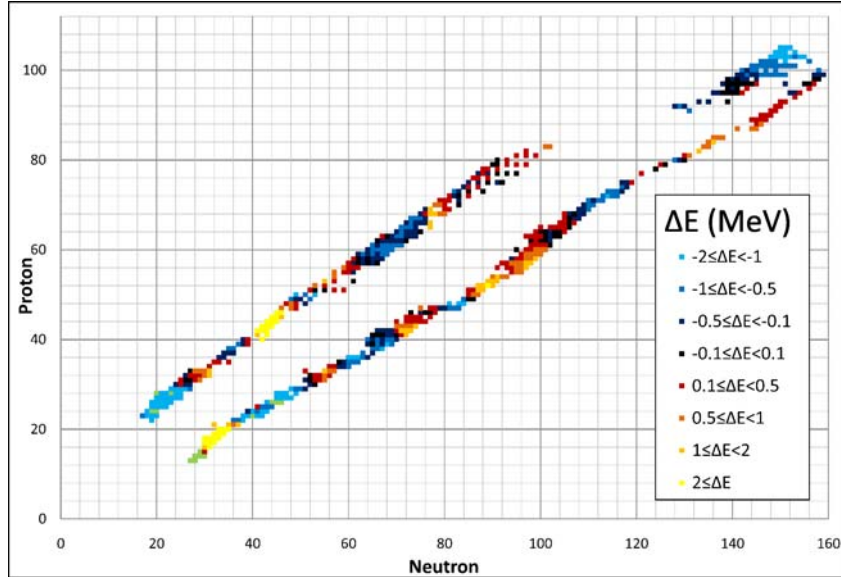


Fig. 9. Difference between the theoretical masses obtained with the formula (8) and 656 2003 AME extrapolated masses.

values are given and compared in Table 4. Without readjustment the formulae (6-8) leads to $\sigma = 0.704$, 0.748 and 0.733 MeV for the 2844 nuclei. When the coefficients are readjusted on these 2844 data the errors are about the same, namely $\sigma = 0.697$, 0.726 and 0.725 MeV, which justifies the adjustment on the most known 2027 nuclei.

8 Summary and conclusion

The coefficients of different macro-microscopic Liquid Drop Model mass formulae including the pairing and shell energies of the Thomas-Fermi model have been determined by an adjustment to 2027 experimental atomic masses. The Coulomb diffuseness correction Z^2/A term or the charge exchange correction $Z^{4/3}/A^{1/3}$ term plays the main role to improve the accuracy of the mass formula. The Wigner term and the curvature energy can also be used separately but their coefficients are very unstable. The remaining differences come probably mainly from the determination of the shell and pairing energies. A rms deviation of 0.54 MeV can be reached between the experimental and theoretical masses. A large constant coefficient $r_0 = 1.22 - 1.23$ fm or a small central radius increasing with the mass can be used. The different fits lead rather to a surface energy coefficient of around 17-18 MeV. Mass predictions of selected expressions have been compared to 161 new experimental masses and the correct agreement allows to provide extrapolations to masses of 656 selected exotic nuclei.

9 Acknowledgments

We thank K. Blaum, M. Block, S. Schwarz and B. Singh for providing us different nuclear mass data.

References

- [1] G. Audi, A.H. Wapstra, C. Thibault, Nucl. Phys. A 729 (2003) 337.
- [2] C.F. von Weizsäcker, Z. Physik 96 (1935) 431.
- [3] H.A. Bethe, R.F. Bacher, Rev. Mod. Phys. 8 (1936) 82.
- [4] P. Möller, J.R. Nix, W.D. Myers, W.J. Swiatecki, At. Data Nucl. Data Tables 59 (1995) 185.
- [5] G. Royer, J. Phys. G 26 (2000) 1149.

- [6] W.D. Myers, W.J. Swiatecki, LBL report 36803, 1994.
- [7] W.D. Myers, W.J. Swiatecki, Nucl. Phys. A 601 (1996) 141.
- [8] M. Samyn, S. Goriely, P.-H. Heenen, J.M. Pearson, F. Tondeur, Nucl. Phys. A 700 (2002) 142.
- [9] J. Rikowska Stone, J. Phys. G 31 (2005) R211.
- [10] S. Goriely, N. Chamel, and J.M. Pearson, Phys. Rev. Lett. 102 (2009) 152503.
- [11] S. Goriely, S. Hilaire, M. Girod, and S. Pru, Phys. Rev. Lett. 109 (2009) 242501.
- [12] J. Duflo and A.P. Zuker, Phys. Rev. C 52 (1995) R1.
- [13] M. Bender, et al., Phys. Lett. B 515 (2001) 42.
- [14] I.O. Morales, J.C. Lopez Vieyra, J.G. Hirsch, and A. Franck, Nucl. Phys. A 828 (2009) 113.
- [15] I. Angeli, At. Data Nucl. Data Tables 87 (2004) 185.
- [16] J. Blocki, J. Randrup, W.J. Swiatecki, C.F. Tsang, Ann. of Physics 105 (1977) 427.
- [17] S. Goriely, M. Samyn, P.-H. Heenen, J.M. Pearson, F. Tondeur, Phys. Rev. C 66 (2002) 024326.
- [18] G. Royer, Nucl. Phys. A 807 (2008) 105.
- [19] W.D. Myers, Nucl. Phys. A 204 (1973) 465.
- [20] G. Royer, B. Remaud, Nucl. Phys. A 444 (1985) 477.
- [21] M.W. Kirson, Nucl. Phys. A 798 (2008) 29.
- [22] A.E.L. Dieperink, P. Van Isacker, Eur. Phys. J. A. 32 (2007) 11.
- [23] K. Pomorski, J. Dudek, Phys. Rev. C 67 (2003) 044316.
- [24] www.nuclearmasses.org, isoltrap.web.cern.ch, www.nndc.bnl.gov and references therein.

Table 4
Theoretical mass excess (in MeV) predicted with the formula (8) and 2003 AME
values for the 656 selected exotic nuclei

Nucleus	E_{th}	E_{AME}	Nucleus	E_{th}	E_{AME}	Nucleus	E_{th}	E_{AME}	Nucleus	E_{th}	E_{AME}	Nucleus	E_{th}	E_{AME}
⁴⁰ Al	26.74	29.3	⁴⁰ V	9.51	10.33	⁴¹ Al	31.96	35.7	⁴¹ Ti	-17.15	-15.7	⁴¹ V	-1.96	-0.21
⁴² Si	13.87	18.43	⁴² V	-9.98	-8.17	⁴² Cr	4.01	5.99	⁴³ Si	22.58	26.7	⁴³ V	-19.75	-18.02
⁴³ Cr	-4.29	-2.13	⁴⁴ Si	30	32.84	⁴⁴ P	9.62	12.1	⁴⁴ Cr	-15.48	-13.46	⁴⁴ Mn	4.47	6.4
⁴⁵ P	18	17.9	⁴⁵ Mn	-7	-5.11	⁴⁵ Fe	11.83	13.58	⁴⁶ Si	2.55	0.7	⁴⁶ Mn	-14.25	-12.37
⁴⁶ Fe	-0.96	0.76	⁴⁷ Si	10.02	8	⁴⁷ Cl	-7.79	-10.52	⁴⁷ Mn	-23.73	-22.26	⁴⁷ Fe	-8.5	-6.62
⁴⁷ Co	9.01	10.7	⁴⁸ Cl	-1.27	-4.7	⁴⁸ Ar	-20.35	-23.72	⁴⁸ Fe	-19.33	-18.16	⁴⁸ Co	0.19	1.64
⁴⁸ Ni	16.33	18.4	⁴⁹ Cl	3.38	0.3	⁴⁹ Ar	-14.07	-18.15	⁴⁹ Fe	-26.14	-24.58	⁴⁹ Co	-10.92	-9.58
⁴⁹ Ni	7.26	9	⁵⁰ Ar	-10.73	-14.5	⁵⁰ Co	-19.02	-17.2	⁵⁰ Ni	-5.1	-3.79	⁵¹ Ar	-3.78	-7.8
⁵¹ K	-19.03	-22	⁵¹ Co	-28.76	-27.27	⁵¹ Ni	-13.47	-11.44	⁵² K	-13.08	-16.2	⁵² Co	-35.27	-33.92
⁵² Ni	-24.49	-22.65	⁵² Cu	-3.75	-2.63	⁵³ K	-8.89	-12	⁵³ Ca	-24.71	-27.9	⁵³ Sc	-36.06	-37.62
⁵³ Ni	-31.36	-29.37	⁵³ Cu	-15.04	-13.46	⁵⁴ Ca	-21.84	-23.89	⁵⁴ Cu	-23.16	-21.69	⁵⁴ Zn	-6.76	-6.57
⁵⁵ Ca	-15.68	-18.12	⁵⁵ Cu	-32.79	-31.62	⁵⁵ Zn	-14.69	-14.92	⁵⁶ Sc	-23.29	-25.27	⁵⁶ Cu	-39.38	-38.6
⁵⁶ Zn	-26.03	-25.73	⁵⁶ Ga	-4.51	-4.74	⁵⁷ Sc	-19.94	-20.69	⁵⁷ Zn	-32.94	-32.8	⁵⁷ Ga	-15.86	-15.9
⁵⁸ Sc	-14.12	-15.17	⁵⁸ Ti	-31.63	-30.77	⁵⁸ Ga	-23.97	-23.99	⁵⁸ Ge	-8.54	-8.37	⁵⁹ Ti	-26.04	-25.22
⁵⁹ Ga	-33.88	-34.12	⁵⁹ Ge	-16.77	-17	⁶⁰ Ti	-23.55	-21.65	⁶⁰ Ga	-39.01	-40	⁶⁰ Ge	-27.56	-27.77
⁶⁰ As	-6.46	-6.4	⁶¹ V	-30.81	-29.36	⁶¹ Ge	-33.35	-33.73	⁶¹ As	-17.5	-18.05	⁶² V	-25.84	-24.42
⁶² Ge	-41.37	-42.24	⁶² As	-24.27	-24.96	⁶³ V	-22.99	-20.91	⁶³ Cr	-35.73	-35.53	⁶³ Ge	-45.63	-46.91
⁶³ As	-32.89	-33.82	⁶⁴ V	-16.6	-15.4	⁶⁴ Cr	-34.7	-33.15	⁶⁴ As	-38.38	-39.52	⁶⁵ V	-13.2	-11.25
⁶⁵ Cr	-28.51	-27.8	⁶⁵ Se	-32.75	-32.92	⁶⁶ Cr	-26.12	-24.8	⁶⁶ Mn	-36.06	36.25	⁶⁷ Cr	-20.28	-19.05
⁶⁷ Mn	-34.32	-33.4	⁶⁷ Br	-32.68	-32.8	⁶⁸ Mn	-29.15	-28.6	⁶⁸ Br	-38.49	-38.64	⁶⁹ Mn	-26.25	-25.3
⁶⁹ Fe	-40.13	-38.4	⁶⁹ Kr	-32.77	-32.44	⁷⁰ Fe	-38.16	-35.9	⁷⁰ Br	-50.93	-51.43	⁷⁰ Kr	-41.57	-41.3
⁷¹ Fe	-33.01	-31	⁷¹ Rb	-32.74	-32.3	⁷² Fe	-30.47	-28.3	⁷² Co	-41.19	-39.3	⁷² Rb	-38.38	-38.12
⁷³ Co	-38.81	-37.04	⁷³ Ni	-51.1	-49.86	⁷³ Rb	-46.26	-46.05	⁷³ Sr	-32.6	-31.7	⁷⁴ Co	-33.99	-32.25
⁷⁴ Ni	-49.54	-48.37	⁷⁴ Sr	-41.69	-40.7	⁷⁵ Co	-31.12	-29.5	⁷⁵ Ni	-45.16	-43.9	⁷⁶ Y	-39.23	-38.7
⁷⁷ Ni	-38.14	-36.75	⁷⁷ Cu	-49.76	-48.58	⁷⁷ Y	-47.24	-46.91	⁷⁸ Cu	-45.6	-44.75	⁷⁸ Y	-52.39	-52.53
⁷⁸ Zr	-41.87	-41.7	⁷⁹ Cu	-43.01	-42.33	⁷⁹ Zr	-46.99	-47.36	⁸⁰ Cu	-36.84	-36.45	⁸² Zn	-42.87	-42.46
⁸² Ga	-53.22	-53.1	⁸² Zr	-61.74	-64.19	⁸² Nb	-51.24	-52.97	⁸³ Zn	-36.29	-36.3	⁸³ Ga	-49.29	-49.39
⁸³ Mo	-44.77	-47.75	⁸⁴ Ga	-43.66	-44.11	⁸⁴ Ge	-58.23	-58.25	⁸⁴ As	-65.86	-66.08	⁸⁴ Nb	-59.24	-61.88
⁸⁴ Mo	-51.32	-55.81	⁸⁵ Ga	-39.65	-40.05	⁸⁵ Ge	-52.63	-53.07	⁸⁵ Mo	-55.51	-59.1	⁸⁵ Tc	-43.65	-47.67
⁸⁶ Ga	-33.4	-34.35	⁸⁶ Ge	-49.47	-49.84	⁸⁶ As	-49.18	-53.21	⁸⁷ Ge	-43.42	-44.24	⁸⁷ Tc	-56.27	-59.12
⁸⁷ Ru	-43.83	-47.34	⁸⁸ Ge	-39.7	-40.14	⁸⁸ As	-50.05	-51.29	⁸⁸ Ru	-52.23	-55.65	⁸⁹ As	-46.5	-47.14
⁸⁹ Ru	-56.81	-59.51	⁸⁹ Rh	-44.7	-47.66	⁹⁰ As	-40.85	-41.45	⁹⁰ Se	-55.62	-55.93	⁹⁰ Rh	-50.51	-53.22
⁹¹ Se	-50.06	-50.34	⁹¹ Rh	-57.83	-59.1	⁹¹ Pd	-44.84	-47.4	⁹² Se	-46.93	-46.65	⁹² Pd	-53.43	-55.5

Table 5
continued...

Nucleus	E_{th}	E_{AME}	Nucleus	E_{th}	E_{AME}	Nucleus	E_{th}	E_{AME}	Nucleus	E_{th}	E_{AME}	Nucleus	E_{th}	E_{AME}
⁹³ Se	-40.99	-40.72	⁹³ Br	-52.98	-53.05	⁹³ Ag	-45.89	-46.78	⁹⁴ Se	-37.48	-36.8	⁹⁴ Br	-48.16	-47.8
⁹⁵ Br	-44.78	-43.9	⁹⁵ Ag	-59.59	-60.1	⁹⁵ Cd	-46.29	-46.7	⁹⁶ Br	-39.51	-38.63	⁹⁶ Kr	-54.29	-53.03
⁹⁶ Ag	-64.41	-64.57	⁹⁶ Cd	-55.2	-56.1	⁹⁷ Br	-35.65	-34.65	⁹⁷ Kr	-49.18	-47.92	⁹⁷ Cd	-60.14	-60.6
⁹⁷ In	-47.8	-47	⁹⁸ Kr	-46.07	-44.8	⁹⁸ In	-54.05	-53.9	⁹⁹ Kr	-40.27	-39.5	⁹⁹ Cd	-70.19	-69.85
⁹⁹ In	-61.76	-61.27	⁹⁹ Sn	-48.27	-47.2	¹⁰⁰ Kr	-36.59	-36.2	¹⁰⁰ Rb	-47.68	-46.7	¹⁰¹ In	-69.51	-68.61
¹⁰¹ Sn	-60.55	-59.56	¹⁰² Rb	-38.75	-38.31	¹⁰³ Sr	-48.49	-47.55	¹⁰³ Y	-59.43	-58.94	¹⁰³ Sn	-68.27	-66.97
¹⁰³ Sb	-56.01	-56.18	¹⁰⁴ Sr	-45.35	-44.4	¹⁰⁴ Y	-54.93	-54.91	¹⁰⁴ Zr	-67.02	-66.34	¹⁰⁴ Sb	-59.08	-59.18
¹⁰⁵ Sr	-39.86	-38.58	¹⁰⁵ Y	-51.87	-51.35	¹⁰⁵ Zr	-62.6	-62.36	¹⁰⁵ Te	-51.73	-52.5	¹⁰⁶ Y	-47.08	-46.77
¹⁰⁶ Zr	-60.21	-59.7	¹⁰⁶ Nb	-67.15	-67.1	¹⁰⁶ Sb	-66.36	-66.33	¹⁰⁷ Y	-43.75	-42.72	¹⁰⁷ Zr	-55.55	-55.19
¹⁰⁷ Nb	-64.86	-64.92	¹⁰⁷ Te	-60.23	-60.54	¹⁰⁸ Y	-38.52	-37.74	¹⁰⁸ Zr	-52.89	-52.2	¹⁰⁸ Nb	-60.77	-60.7
¹⁰⁸ Mo	-71.41	-71.3	¹⁰⁸ Sb	-72.34	-72.51	¹⁰⁸ I	-51.61	-52.65	¹⁰⁹ Zr	-47.81	-47.28	¹⁰⁹ Nb	-58.23	-58.1
¹⁰⁹ Mo	-67.46	-67.25	¹¹⁰ Zr	-44.37	-43.9	¹¹⁰ Nb	-53.82	-53.62	¹¹⁰ Mo	-65.62	-65.46	¹¹⁰ Sb	-77.33	-77.54
¹¹⁰ I	-59.83	-60.32	¹¹¹ Nb	-50.55	-50.63	¹¹¹ Mo	-61.29	-61.1	¹¹¹ Xe	-53.65	-54.4	¹¹² Nb	-45.4	-45.8
¹¹² Mo	-58.7	-58.83	¹¹² Cs	-45.39	-46.29	¹¹³ Nb	-40.87	-42.2	¹¹³ Mo	-52.99	-54.14	¹¹³ Tc	-63.04	-63.72
¹¹⁴ Mo	-50.24	-51.31	¹¹⁴ Tc	-58.81	-59.73	¹¹⁴ Ru	-70.36	-70.53	¹¹⁴ I	-72.75	-72.8	¹¹⁴ Cs	-54.31	-54.54
¹¹⁵ Mo	-45.21	-46.31	¹¹⁵ Tc	-56.16	-57.11	¹¹⁵ Cs	-59.48	-59.7	¹¹⁵ Ba	-48.2	-49.03	¹¹⁶ Tc	-51.75	-52.75
¹¹⁶ Ru	-64.22	-64.45	¹¹⁶ Cs	-62.26	-62.07	¹¹⁶ Ba	-54.23	-54.6	¹¹⁷ Tc	-48.74	-49.85	¹¹⁷ Ru	-59.9	-60.01
¹¹⁷ Rh	-68.74	-68.95	¹¹⁷ Ba	-57.18	-57.29	¹¹⁷ La	-46.25	-46.51	¹¹⁸ Ru	-57.59	-57.92	¹¹⁸ Rh	-65.02	-65.14
¹¹⁸ Ba	-62.17	-62.37	¹¹⁸ La	-49.9	-49.62	¹¹⁹ Ru	-53.11	-53.24	¹¹⁹ Rh	-62.81	-63.24	¹¹⁹ Pd	-71.64	-71.62
¹¹⁹ La	-55.06	-54.97	¹¹⁹ Ce	-43.89	-44	¹²⁰ Ru	-50.46	-50.94	¹²⁰ Rh	-58.98	-59.23	¹²⁰ La	-57.91	-57.69
¹²⁰ Ce	-49.77	-49.71	¹²¹ Pd	-66.45	-66.26	¹²¹ La	-62.36	-62.4	¹²¹ Ce	-52.82	-52.7	¹²¹ Pr	-41.75	-41.58
¹²² Rh	-52.46	-52.9	¹²² Pd	-64.62	-64.69	¹²² Ag	-70.67	-71.23	¹²² La	-64.78	-64.54	¹²² Ce	-57.94	-57.84
¹²² Pr	-45.47	-44.89	¹²³ Pd	-60.56	-60.61	¹²³ La	-68.76	-68.71	¹²³ Ce	-60.43	-60.18	¹²³ Pr	-50.66	-50.34
¹²⁴ Pd	-58.67	-58.8	¹²⁴ Ag	-66.11	-66.47	¹²⁴ Ce	-64.99	-64.82	¹²⁴ Pr	-53.77	-53.13	¹²⁴ Nd	-44.97	-44.5
¹²⁵ Ag	-64.61	-64.8	¹²⁵ Ce	-66.96	-66.66	¹²⁵ Pr	-58.4	-57.91	¹²⁵ Nd	-48.15	-47.62	¹²⁶ Ag	-61.15	-61.01
¹²⁶ Pr	-60.96	-60.26	¹²⁶ Nd	-53.41	-52.89	¹²⁶ Pm	-40.11	-39.57	¹²⁷ Ag	-59.22	-58.9	¹²⁷ Pr	-65.01	-64.43
¹²⁷ Nd	-56.08	-55.42	¹²⁷ Pm	-45.47	-45.06	¹²⁸ Ag	-55.78	-54.8	¹²⁸ Nd	-60.74	-60.18	¹²⁸ Pm	-48.74	-48.05
¹²⁸ Sm	-39.02	-39.05	¹²⁹ Ag	-53.19	-52.45	¹²⁹ Cd	-64.6	-63.2	¹²⁹ Nd	-62.84	-62.24	¹²⁹ Pm	-53.51	-52.95
¹²⁹ Sm	-42.38	-42.25	¹³⁰ Ag	-47.01	-46.16	¹³⁰ Pm	-56.22	-55.47	¹³⁰ Sm	-47.84	-47.58	¹³⁰ Eu	-33.74	-33.94
¹³¹ Cd	-56.48	-55.27	¹³¹ Pm	-60.3	-59.74	¹³¹ Sm	-50.63	-50.2	¹³¹ Eu	-39.4	-39.35	¹³² Cd	-51.97	-50.72
¹³² Pm	-62.39	-61.71	¹³² Sm	-55.48	-55.25	¹³² Eu	-42.9	-42.5	¹³³ In	-58.43	-57.93	¹³³ Sm	-57.57	-57.13
¹³³ Eu	-47.85	-47.28	¹³⁴ In	-52.04	-52.02	¹³⁴ Sm	-61.57	-61.51	¹³⁴ Eu	-50.54	-49.83	¹³⁴ Gd	-41.9	-41.57
¹³⁵ In	-47.13	-47.2	¹³⁵ Sn	-60.42	-60.8	¹³⁵ Eu	-54.65	-54.19	¹³⁵ Gd	-44.72	-44.18	¹³⁶ Sn	-56	-56.5

Table 6
continued...

Nucleus	E_{th}	E_{AME}	Nucleus	E_{th}	E_{AME}	Nucleus	E_{th}	E_{AME}	Nucleus	E_{th}	E_{AME}	Nucleus	E_{th}	E_{AME}
¹³⁶ Sb	-64.44	-64.88	¹³⁶ Eu	-56.69	-56.26	¹³⁶ Gd	-49.44	-49.05	¹³⁶ Tb	-36.76	-35.97	¹³⁷ Sn	-49.45	-50.31
¹³⁷ Sb	-60.13	-60.26	¹³⁷ Eu	-60.19	-60.02	¹³⁷ Gd	-51.59	-51.21	¹³⁷ Tb	-41.53	-41	¹³⁸ Sb	-53.44	-55.15
¹³⁸ Gd	-55.91	-55.78	¹³⁸ Tb	-44.27	-43.63	¹³⁸ Dy	-35.39	-34.94	¹³⁹ Sb	-49.13	-50.32	¹³⁹ Te	-59.43	-60.8
¹³⁹ Gd	-57.62	-57.53	¹³⁹ Tb	-48.5	-48.17	¹³⁹ Dy	-38.31	-37.69	¹⁴⁰ Te	-55.61	-56.96	¹⁴⁰ Dy	-43.22	-42.84
¹⁴⁰ Ho	-30.08	-29.31	¹⁴¹ Te	-49.4	-51.56	¹⁴¹ Dy	-45.65	-45.32	¹⁴¹ Ho	-34.92	-34.37	¹⁴² Te	-45.55	-47.43
¹⁴² I	-53.75	-55.72	¹⁴² Tb	-55.88	-57.06	¹⁴² Dy	-50.13	-49.96	¹⁴² Ho	-38.15	-37.47	¹⁴³ I	-50.08	-51.64
¹⁴³ Dy	-51.14	-52.32	¹⁴³ Ho	-42.62	-42.28	¹⁴³ Er	-31.55	-31.35	¹⁴⁴ I	-44.58	-46.58	¹⁴⁴ Xe	-56.46	-57.28
¹⁴⁴ Er	-36.59	-36.91	¹⁴⁵ Xe	-51.08	-52.1	¹⁴⁵ Er	-38.24	-39.69	¹⁴⁵ Tm	-28.17	-27.88	¹⁴⁶ Xe	-47.9	-48.67
¹⁴⁶ Er	-43.62	-44.71	¹⁴⁶ Tm	-30.24	-31.28	¹⁴⁷ Xe	-42.54	-43.26	¹⁴⁷ Ba	-60.26	-60.6	¹⁴⁷ Er	-46.3	-47.05
¹⁴⁸ Er	-51.07	-51.65	¹⁴⁸ Yb	-29.51	-30.35	¹⁴⁹ Cs	-43.41	-43.85	¹⁴⁹ Ba	-53.16	-53.49	¹⁴⁹ La	-60.66	-60.8
¹⁴⁹ Tm	-43.79	-44.04	¹⁴⁹ Yb	-32.86	-33.5	¹⁵⁰ Cs	-38.29	-38.96	¹⁵⁰ Ba	-50.12	-50.6	¹⁵⁰ La	-56.7	-57.04
¹⁵⁰ Tm	-46.42	-46.61	¹⁵⁰ Yb	-38.32	-38.73	¹⁵⁰ Lu	-24.45	-24.94	¹⁵¹ Cs	-34.34	-35.22	¹⁵¹ Ba	-45.15	-45.82
¹⁵¹ La	-53.76	-54.29	¹⁵¹ Lu	-29.94	-30.2	¹⁵² Ba	-41.72	-42.6	¹⁵² La	-49.34	-50.07	¹⁵² Ce	-59.26	-59.11
¹⁵² Lu	-33.18	-33.42	¹⁵³ Ba	-36.48	-37.62	¹⁵³ La	-46.02	-46.93	¹⁵³ Ce	-54.97	-55.35	¹⁵³ Yb	-47.09	-47.06
¹⁵³ Hf	-26.82	-27.3	¹⁵⁴ La	-41.3	-42.38	¹⁵⁴ Ce	-52.25	-52.7	¹⁵⁴ Lu	-39.88	-39.57	¹⁵⁴ Hf	-32.87	-32.73
¹⁵⁵ La	-37.71	-38.8	¹⁵⁵ Ce	-47.65	-48.4	¹⁵⁵ Pr	-55.37	-55.78	¹⁵⁵ Nd	-62.38	-62.47	¹⁵⁵ Hf	-34.18	-34.1
¹⁵⁵ Ta	-24.38	-23.67	¹⁵⁶ Ce	-44.6	-45.4	¹⁵⁶ Pr	-51.28	-51.91	¹⁵⁶ Ta	-26.2	-25.8	¹⁵⁷ Ce	-39.66	-40.67
¹⁵⁷ Pr	-48.29	-48.97	¹⁵⁷ Nd	-56.36	-56.79	¹⁵⁷ Hf	-38.54	-38.75	¹⁵⁸ Pr	-43.86	-44.73	¹⁵⁸ Nd	-53.94	-54.4
¹⁵⁸ Ta	-31.1	-31.02	¹⁵⁸ W	-23.81	-23.7	¹⁵⁹ Pr	-40.68	-41.45	¹⁵⁹ Nd	-49.6	-50.22	¹⁵⁹ Pm	-56.5	-56.85
¹⁵⁹ W	-24.99	-25.23	¹⁶⁰ Nd	-46.91	-47.42	¹⁶⁰ Pm	-52.73	-53.1	¹⁶⁰ Sm	-60.5	-60.42	¹⁶⁰ Eu	-63.14	-63.37
¹⁶⁰ Re	-16.95	-16.66	¹⁶¹ Nd	-42.36	-42.96	¹⁶¹ Pm	-50.12	-50.43	¹⁶¹ Sm	-56.88	-56.98	¹⁶¹ Eu	-61.57	-61.78
¹⁶¹ Ta	-38.7	-38.73	¹⁶¹ W	-30.08	-30.41	¹⁶² Pm	-46.07	-46.31	¹⁶² Sm	-54.8	-54.75	¹⁶² Eu	-58.43	-58.65
¹⁶² Re	-22.54	-22.35	¹⁶² Os	-14.13	-14.5	¹⁶³ Pm	-43.07	-43.15	¹⁶³ sm	-50.83	-50.9	¹⁶³ Eu	-56.47	-56.63
¹⁶³ Gd	-61.17	-61.49	¹⁶³ Os	-15.9	-16.12	¹⁶⁴ Sm	-48.36	-48.18	¹⁶⁴ Eu	-53.02	-53.1	¹⁶⁴ Gd	-59.76	-59.75
¹⁶⁴ Re	-27.54	-27.64	¹⁶⁴ Ir	-7.55	-7.27	¹⁶⁵ Eu	-50.66	-50.56	¹⁶⁵ Gd	-56.41	-56.47	¹⁶⁵ Tb	-60.27	-60.66
¹⁶⁵ Os	-21.43	-21.65	¹⁶⁵ Ir	-11.32	-11.63	¹⁶⁶ Eu	-46.68	-46.6	¹⁶⁶ Gd	-54.52	-54.4	¹⁶⁶ Re	-31.99	-31.85
¹⁶⁶ Ir	-13.32	-13.21	¹⁶⁶ Pt	-4.35	-4.79	¹⁶⁷ Eu	-43.65	-43.59	¹⁶⁷ Gd	-50.67	-50.7	¹⁶⁷ Tb	-55.69	-55.84
¹⁶⁷ Re	-34.75	-34.84	¹⁶⁷ Pt	-6.17	-6.54	¹⁶⁸ Gd	-48.17	-48.1	¹⁶⁸ Tb	-52.35	-52.5	¹⁶⁸ Ir	-18.73	-18.74
¹⁶⁹ Gd	-43.71	-43.9	¹⁶⁹ Tb	-49.99	-50.1	¹⁶⁹ Pt	-12.03	-12.38	¹⁶⁹ Au	-1.71	-1.79	¹⁷⁰ Tb	-46.13	-46.34
¹⁷⁰ Dy	-53.49	-53.66	¹⁷⁰ Ir	-23.4	-23.32	¹⁷⁰ Au	-3.7	-3.61	¹⁷¹ Tb	-43.48	-43.5	¹⁷¹ Dy	-49.76	-50.11
¹⁷¹ Hg	3.57	3.5	¹⁷² Dy	-47.65	-47.73	¹⁷² Ho	-51.09	-51.4	¹⁷² Ir	-27.48	-27.52	¹⁷² Au	-9.06	-9.28
¹⁷³ Dy	-43.62	-43.78	¹⁷³ Ho	-49.11	-49.1	¹⁷³ Er	-53.54	-53.65	¹⁷³ Hg	-2.31	-2.57	¹⁷⁴ Ho	-45.65	-45.5
¹⁷⁴ Er	-52.09	-51.95	¹⁷⁴ Au	-13.87	-14.2	¹⁷⁵ Ho	-43.25	-42.8	¹⁷⁵ Er	-48.73	-48.65	¹⁷⁶ Er	-46.89	-46.5

Table 7
continued...

Nucleus	E_{th}	E_{AME}	Nucleus	E_{th}	E_{AME}	Nucleus	E_{th}	E_{AME}	Nucleus	E_{th}	E_{AME}	Nucleus	E_{th}	E_{AME}
¹⁷⁶ Au	-18.14	-18.54	¹⁷⁶ Tl	0.87	0.55	¹⁷⁷ Er	-43.06	-42.8	¹⁷⁷ Tm	-47.76	-47.47	¹⁷⁸ Tm	-44.44	-44.12
¹⁷⁸ Tl	-4.38	-4.75	¹⁷⁹ Tm	-42.19	-41.6	¹⁷⁹ Yb	-46.88	-46.42	¹⁷⁹ Pb	2.34	2	¹⁸⁰ Yb	-45.15	-44.4
¹⁸⁰ Tl	-9.07	-9.4	¹⁸¹ Yb	-41.58	-40.85	¹⁸¹ Lu	-45.29	-44.74	¹⁸² Lu	-42.24	-41.88	¹⁸³ Lu	-40.21	-39.52
¹⁸⁴ Lu	-37.01	-36.41	¹⁸⁴ Bi	1.88	1.05	¹⁸⁵ Hf	-39.06	-38.36	¹⁸⁵ Bi	-1.47	-2.21	¹⁸⁶ Hf	-37.44	-36.43
¹⁸⁷ Hf	-33.9	-32.98	¹⁸⁷ Ta	-37.73	-36.77	¹⁸⁸ Hf	-31.73	-30.88	¹⁸⁸ Ta	-34.59	-33.81	¹⁸⁹ Ta	-32.55	-31.83
¹⁹⁰ Ta	-29	-28.66	¹⁹¹ W	-31.72	-31.11	¹⁹² W	-29.98	-29.65	¹⁹² Re	-32.1	-31.71	¹⁹³ Re	-30.48	-30.3
¹⁹⁴ Re	-27.15	-27.55	¹⁹⁸ Ir	-25.39	-25.82	²⁰² Pt	-22.66	-22.6	²⁰⁴ Au	-20.5	-20.75	²⁰⁵ Au	-18.8	-18.75
²⁰⁸ Hg	-13.62	-13.1	²⁰⁹ Hg	-8.54	-8.35	²¹⁰ Hg	-5.14	-5.11	²¹¹ Tl	-5.61	-6.08	²¹² tl	-0.84	-1.65
²¹⁵ Pb	5.67	4.48	²¹⁷ Bi	9.78	8.82	²¹⁸ Bi	14.28	13.34	²¹⁹ Po	13.72	12.8	²²⁰ Po	16.51	15.47
²²⁰ U	22.6	23.03	²²¹ At	17.4	16.81	²²¹ U	24.05	24.59	²²² At	21.58	20.8	²²² Pa	21.27	22.12
²²² U	24.17	24.3	²²³ At	24.39	23.46	²²⁶ Np	32.44	32.74	²²⁸ Fr	34.05	33.28	²²⁸ Np	33.5	33.7
²³¹ Fr	43.04	42.33	²³¹ Am	42.09	42.44	²³² Fr	46.99	46.36	²³² Np	37.42	37.36	²³² Am	43.16	43.4
²³³ Ra	45.18	44.77	²³³ Ac	41.91	41.5	²³³ Am	43.11	43.17	²³⁴ Ra	47.81	47.23	²³⁴ Ac	45.49	45.1
²³⁴ Am	44.43	44.53	²³⁵ Ac	48.09	47.72	²³⁵ Am	44.62	44.66	²³⁵ Cm	47.98	47.91	²³⁵ Bk	52.44	52.7
²³⁶ Ac	51.75	51.51	²³⁶ Th	46.8	46.45	²³⁶ Am	46.25	46.18	²³⁶ Cm	47.75	47.89	²³⁶ Bk	53.32	53.4
²³⁷ Th	50.42	50.2	²³⁷ Am	46.79	46.57	²³⁷ Cm	49.36	49.28	²³⁷ Bk	53.04	53.1	²³⁷ cf	57.73	57.82
²³⁸ Th	52.88	52.63	²³⁸ Bk	54.27	54.29	²³⁸ Cf	57.05	57.2	²³⁹ Pa	53.64	53.34	²³⁹ Cm	51.4	51.19
²³⁹ Bk	54.28	54.29	²³⁹ Cf	58.24	58.15	²⁴⁰ Pa	57.27	56.8	²⁴⁰ Bk	55.66	55.67	²⁴⁰ Cf	57.85	58.03
²⁴⁰ Es	63.9	64.2	²⁴¹ U	56.49	56.2	²⁴¹ Bk	56.12	56.1	²⁴¹ Cf	59.16	59.36	²⁴¹ Es	63.39	63.84
²⁴² U	58.8	58.62	²⁴² Bk	57.91	57.74	²⁴² Es	64.44	64.97	²⁴² Fm	67.88	68.4	²⁴³ Np	59.98	59.88
²⁴³ Cf	60.72	60.95	²⁴³ Es	64.44	64.78	²⁴³ Fm	68.88	69.26	²⁴⁴ Np	63.5	63.2	²⁴⁴ Es	65.53	66.03
²⁴⁴ Fm	68.45	69.01	²⁴⁵ Es	65.82	66.44	²⁴⁵ Fm	69.49	70.22	²⁴⁵ Md	74.78	75.29	²⁴⁶ Es	67.39	67.9
²⁴⁶ Md	75.71	76.28	²⁴⁷ Pu	69.11	69	²⁴⁷ Am	66.85	67.15	²⁴⁷ Es	67.96	68.61	²⁴⁷ Fm	70.89	71.58
²⁴⁷ Md	75.27	76.04	²⁴⁸ Am	70.43	70.56	²⁴⁸ Bk	67.76	68.08	²⁴⁸ Es	69.79	70.3	²⁴⁸ Md	76.37	77.15
²⁴⁸ No	79.81	80.66	²⁴⁹ Am	73.26	73.1	²⁴⁹ Es	70.62	71.18	²⁴⁹ Fm	72.82	73.62	²⁴⁹ Md	76.46	77.33
²⁴⁹ No	80.9	81.82	²⁵⁰ Es	72.57	73.23	²⁵⁰ Md	77.84	78.64	²⁵⁰ No	80.58	81.52	²⁵¹ Md	78.15	79.03
²⁵¹ No	81.91	82.91	²⁵¹ Lr	86.76	87.9	²⁵² Cm	79.3	79.06	²⁵² Bk	78.59	78.53	²⁵² Md	79.67	80.63
²⁵² Lr	87.72	88.84	²⁵³ Bk	80.96	80.93	²⁵³ Md	80.42	81.3	²⁵³ No	83.38	84.47	²⁵³ Lr	87.48	88.69
²⁵³ Rf	92.61	93.79	²⁵⁴ Bk	84.74	84.39	²⁵⁴ Md	82.89	83.51	²⁵⁴ Lr	88.69	89.85	²⁵⁴ Rf	92	93.32
²⁵⁵ Cf	84.81	84.81	²⁵⁵ Lr	88.81	90.06	²⁵⁵ Rf	93.03	94.4	²⁵⁵ Db	98.47	100.04	²⁵⁶ Cf	87.11	87.04
²⁵⁶ Es	87.01	87.19	²⁵⁶ Lr	90.89	91.87	²⁵⁶ Db	99.14	100.72	²⁵⁷ Es	89.14	89.4	²⁵⁷ Lr	91.64	92.74
²⁵⁷ Rf	94.86	95.93	²⁵⁷ Db	98.94	100.34	²⁵⁸ Es	92.54	92.7	²⁵⁸ Fm	89.92	90.43	²⁵⁸ No	90.83	91.48
²⁵⁸ Lr	93.83	94.84												